Relativistic many-body calculations of energies of $n=3$ states in aluminumlike ions

U. I. Safronova,[1,2] C. Namba,[1] J. R. Albritton,[3] W. R. Johnson,[2] and M. S. Safronova[2]
[1]*National Institute for Fusion Science, Toki, Gifu, 509-5292, Japan*
[2]*Department of Physics, University of Notre Dame, Notre Dame, Indiana 46556*
[3]*Lawrence Livermore National Laboratory, P. O. Box 808, Livermore, California 94551*

(Received 26 June 2001; revised manuscript received 24 August 2001; published 11 January 2002)

Energies of $3l3l'3l''$ states of aluminumlike ions with $Z=14$–100 are evaluated to second order in relativistic many-body perturbation theory starting from a $1s^22s^22p^6$ Dirac-Fock potential. Intrinsic three-particle contributions to the energy are included in the present calculation and found to contribute about 10–20 % of the total second-order energy. Corrections for the frequency-dependent Breit interaction and the Lamb shift are included in lowest order. A detailed discussion of contributions to the energy levels is given for aluminumlike germanium $(Z=32)$. Comparisons are made with available experimental data. We obtain excellent agreement for term splitting, even for low-Z ions. These calculations are presented as a theoretical benchmark for comparison with experiment and theory.

DOI: 10.1103/PhysRevA.65.022507 PACS number(s): 32.30.Rj, 32.70.Cs, 31.25.Jf, 31.15.Md

I. INTRODUCTION

Ions of the aluminum isoelectronic sequence have three valence electrons outside a closed $n=2$ core and provide a model for studying effects of strong correlation on closely spaced levels in heavy atoms. There are many examples in the Al sequence of level crossings of states having the same parity and angular momentum; such examples occur for both low and high values of the nuclear charge Z. Notably, the $3s3p^2$, $3s3p3d$, and $3p^3$ levels cross the $3s^2nl$ $(l=0$ to 4) levels, becoming relatively more tightly bound as the nuclear charge Z increases. Such crossings provide stringent tests of atomic structure calculations. Comparisons with measurements of energies, transition rates, and fine-structure intervals also provide useful tests of the quality of different theoretical models. Many experimental energy levels and fine-structure intervals are now available up to very high nuclear charge $(Z=40)$ for $3l3l'3l''$ levels; additionally, experimental rates for some transitions between these levels are available. The objective of this paper is to present a comprehensive set of calculations for $3l3l'3l''$ energies to compare with previous calculations and experiments for the entire Al isoelectronic sequence. Most earlier measurements and calculations focused on $3s^23p\ ^2P^o$ states and low-lying $3s3p^2\ ^4P^e$ levels. Very few results exist for other $3s^23d$, $3s3p3d$, and $3p^3$ states. The large number of possible transitions have made experimental identification difficult. Experimental verifications should become simpler and more reliable using this more accurate set of calculations.

Several early theoretical calculations for Al-like ions were based on the Hartree-Fock method: excitation energies and line strengths for low-lying states of ions in the sequence were studied using multiconfiguration Dirac-Fock wave functions by Huang [1] and oscillator strengths were evaluated using multiconfiguration Hartree-Fock wave functions by Fawcett [2]. Wavelengths, oscillator strengths, and transition probabilities for electric-dipole transitions between low-lying levels of the Al-like ions were calculated using a relativistic parametric potential by Farrag *et al.* in Ref. [3].

In the present paper, we use relativistic many-body perturbation theory (MBPT) to determine energies of $n=3$ states for aluminumlike ions with nuclear charges in the range $Z=14$–100. We illustrate our calculation with detailed studies of the case of aluminumlike germanium $(Z=32)$. Our calculations are carried out to second order in perturbation theory and include one-particle, two-particle, and three-particle contributions to the energy. Three-particle contributions account for 10–20 % of the total second-order energy. The frequency-dependent Breit interaction is included in first order. Finally, QED corrections are included using the screened self-energy and vacuum polarization data given by Blundell [4].

Our perturbation theory calculations are carried out using single-particle orbitals calculated in the Hartree-Fock potential of the $1s^22s^22p^6$ neonlike core. As a first step, we determine and store the single-particle contributions to the energies of the five $n=3$ states $3s$, $3p_{1/2}$, $3p_{3/2}$, $3d_{3/2}$, and $3d_{5/2}$ in lowest, first, and second orders. These contributions are precisely those needed to calculate energies of $n=3$ states of sodiumlike ions. Next, we evaluate the 155 two-particle matrix elements of the effective Hamiltonian $\langle 3l3l'\ J|H^{\rm eff}|3l''3l'''\ J\rangle$ in first and second orders. These two-particle matrix elements are identical to those used in Ref. [5] to evaluate energies of the $3l3l'$ levels for magnesiumlike ions. Finally, second-order (intrinsic) three-particle matrix elements are evaluated. Combining the one-, two-, and three-particle matrix elements using the method given in Refs. [6,7], we calculate one-, two-, and three-particle contributions to the energies of aluminumlike ions.

The MBPT energies evaluated here compare well with predicted energies based on experimental measurements given in Refs. [8–23]. Multiplet splittings along the isoelectronic sequence are evaluated and agree to three digits with available experimental data for most cases.

II. METHOD

The MBPT formalism developed previously in Refs. [6,7] for B-like ions is used here to obtain second-order energies for Al-like ions. Differences between calculations for B-like

TABLE I. Possible three-particle states in the $n=3$ complex in the jj-coupling scheme.

$J=1/2$	$J=3/2$	$J=5/2$	$J=7/2$–$11/2$
	Odd-parity states		
$3s_{1/2}3s_{1/2}[0]3p_{1/2}$	$3s_{1/2}3s_{1/2}[0]3p_{3/2}$	$3p_{3/2}3p_{3/2}[2]3p_{1/2}$	$3s_{1/2}3p_{1/2}[1]3d_{5/2}$
$3p_{3/2}3p_{3/2}[0]3p_{1/2}$	$3p_{3/2}3p_{3/2}[2]3p_{1/2}$	$3s_{1/2}3p_{1/2}[0]3d_{5/2}$	$3s_{1/2}3p_{3/2}[1]3d_{5/2}$
$3s_{1/2}3p_{1/2}[1]3d_{3/2}$	$3p_{1/2}3p_{1/2}[0]3p_{3/2}$	$3s_{1/2}3p_{1/2}[1]3d_{3/2}$	$3s_{1/2}3p_{3/2}[2]3d_{3/2}$
$3s_{1/2}3p_{3/2}[1]3d_{3/2}$	$3p_{3/2}3p_{3/2}[0]3p_{3/2}$	$3s_{1/2}3p_{1/2}[1]3d_{5/2}$	$3s_{1/2}3p_{3/2}[2]3d_{5/2}$
$3s_{1/2}3p_{3/2}[2]3d_{3/2}$	$3s_{1/2}3p_{1/2}[0]3d_{3/2}$	$3s_{1/2}3p_{3/2}[1]3d_{3/2}$	$3d_{3/2}3d_{3/2}[2]3p_{3/2}$
$3s_{1/2}3p_{3/2}[2]3d_{5/2}$	$3s_{1/2}3p_{1/2}[1]3d_{3/2}$	$3s_{1/2}3p_{3/2}[1]3d_{5/2}$	$3d_{5/2}3d_{5/2}[2]3p_{3/2}$
$3d_{3/2}3d_{3/2}[0]3p_{1/2}$	$3s_{1/2}3p_{1/2}[1]3d_{5/2}$	$3s_{1/2}3p_{3/2}[2]3d_{3/2}$	$3d_{5/2}3d_{5/2}[4]3p_{1/2}$
$3d_{3/2}3d_{3/2}[2]3p_{3/2}$	$3s_{1/2}3p_{3/2}[1]3d_{3/2}$	$3s_{1/2}3p_{3/2}[2]3d_{5/2}$	$3d_{5/2}3d_{5/2}[4]3p_{3/2}$
$3d_{5/2}3d_{5/2}[0]3p_{1/2}$	$3s_{1/2}3p_{3/2}[1]3d_{5/2}$	$3d_{3/2}3d_{3/2}[2]3p_{1/2}$	$3d_{3/2}3d_{5/2}[2]3p_{3/2}$
$3d_{5/2}3d_{5/2}[2]3p_{3/2}$	$3s_{1/2}3p_{3/2}[2]3d_{3/2}$	$3d_{3/2}3d_{3/2}[2]3p_{3/2}$	$3d_{3/2}3d_{5/2}[3]3p_{1/2}$
$3d_{3/2}3d_{5/2}[1]3p_{1/2}$	$3s_{1/2}3p_{3/2}[2]3d_{5/2}$	$3d_{5/2}3d_{5/2}[2]3p_{1/2}$	$3d_{3/2}3d_{5/2}[3]3p_{3/2}$
$3d_{3/2}3d_{5/2}[1]3p_{3/2}$	$3d_{3/2}3d_{3/2}[0]3p_{3/2}$	$3d_{5/2}3d_{5/2}[2]3p_{3/2}$	$3d_{3/2}3d_{5/2}[4]3p_{1/2}$
$3d_{3/2}3d_{5/2}[2]3p_{3/2}$	$3d_{3/2}3d_{3/2}[2]3p_{1/2}$	$3d_{5/2}3d_{5/2}[4]3p_{3/2}$	$3d_{3/2}3d_{5/2}[4]3p_{3/2}$
	$3d_{3/2}3d_{3/2}[2]3p_{3/2}$	$3d_{3/2}3d_{5/2}[1]3p_{3/2}$	
	$3d_{5/2}3d_{5/2}[0]3p_{3/2}$	$3d_{3/2}3d_{5/2}[2]3p_{1/2}$	$3s_{1/2}3p_{3/2}[2]3d_{5/2}$
	$3d_{5/2}3d_{5/2}[2]3p_{1/2}$	$3d_{3/2}3d_{5/2}[2]3p_{3/2}$	$3d_{5/2}3d_{5/2}[4]3p_{1/2}$
	$3d_{5/2}3d_{5/2}[2]3p_{3/2}$	$3d_{3/2}3d_{5/2}[3]3p_{1/2}$	$3d_{5/2}3d_{5/2}[4]3p_{3/2}$
	$3d_{3/2}3d_{5/2}[1]3p_{1/2}$	$3d_{3/2}3d_{5/2}[3]3p_{3/2}$	$3d_{3/2}3d_{5/2}[3]3p_{3/2}$
	$3d_{3/2}3d_{5/2}[1]3p_{3/2}$	$3d_{3/2}3d_{5/2}[4]3p_{3/2}$	$3d_{3/2}3d_{5/2}[4]3p_{1/2}$
	$3d_{3/2}3d_{5/2}[2]3p_{1/2}$		$3d_{3/2}3d_{5/2}[4]3p_{3/2}$
	$3d_{3/2}3d_{5/2}[2]3p_{3/2}$		
	$3d_{3/2}3d_{5/2}[3]3p_{3/2}$		$3d_{5/2}3d_{5/2}[4]3p_{3/2}$
			$3d_{3/2}3d_{5/2}[4]3p_{3/2}$
	Even-parity states		
$3p_{1/2}3p_{1/2}[0]3s_{1/2}$	$3p_{1/2}3p_{3/2}[1]3s_{1/2}$	$3p_{1/2}3p_{3/2}[2]3s_{1/2}$	$3p_{3/2}3p_{3/2}[2]3d_{3/2}$
$3p_{3/2}3p_{3/2}[0]3s_{1/2}$	$3p_{1/2}3p_{3/2}[2]3s_{1/2}$	$3p_{3/2}3p_{3/2}[2]3s_{1/2}$	$3p_{3/2}3p_{3/2}[2]3d_{5/2}$
$3p_{1/2}3p_{3/2}[1]3s_{1/2}$	$3p_{3/2}3p_{3/2}[2]3s_{1/2}$	$3s_{1/2}3s_{1/2}[0]3d_{5/2}$	$3p_{1/2}3p_{3/2}[1]3d_{5/2}$
$3p_{3/2}3p_{3/2}[2]3d_{3/2}$	$3s_{1/2}3s_{1/2}[0]3d_{3/2}$	$3p_{1/2}3p_{1/2}[0]3d_{5/2}$	$3p_{1/2}3p_{3/2}[2]3d_{3/2}$
$3p_{3/2}3p_{3/2}[2]3d_{5/2}$	$3p_{1/2}3p_{1/2}[0]3d_{3/2}$	$3p_{3/2}3p_{3/2}[0]3d_{5/2}$	$3p_{1/2}3p_{3/2}[2]3d_{5/2}$
$3p_{1/2}3p_{3/2}[1]3d_{3/2}$	$3p_{3/2}3p_{3/2}[0]3d_{3/2}$	$3p_{3/2}3p_{3/2}[2]3d_{3/2}$	$3d_{5/2}3d_{5/2}[4]3s_{1/2}$
$3p_{1/2}3p_{3/2}[2]3d_{3/2}$	$3p_{3/2}3p_{3/2}[2]3d_{3/2}$	$3p_{3/2}3p_{3/2}[2]3d_{5/2}$	$3d_{3/2}3d_{5/2}[3]3s_{1/2}$
$3p_{1/2}3p_{3/2}[2]3d_{5/2}$	$3p_{3/2}3p_{3/2}[2]3d_{5/2}$	$3p_{1/2}3p_{3/2}[1]3d_{3/2}$	$3d_{3/2}3d_{5/2}[4]3s_{1/2}$
$3d_{3/2}3d_{3/2}[0]3s_{1/2}$	$3p_{1/2}3p_{3/2}[1]3d_{3/2}$	$3p_{1/2}3p_{3/2}[1]3d_{5/2}$	$3d_{3/2}3d_{3/2}[2]3d_{5/2}$
$3d_{5/2}3d_{5/2}[0]3s_{1/2}$	$3p_{1/2}3p_{3/2}[1]3d_{5/2}$	$3p_{1/2}3p_{3/2}[2]3d_{3/2}$	$3d_{5/2}3d_{5/2}[2]3d_{3/2}$
$3d_{3/2}3d_{5/2}[1]3s_{1/2}$	$3p_{1/2}3p_{3/2}[2]3d_{3/2}$	$3p_{1/2}3p_{3/2}[2]3d_{5/2}$	$3d_{5/2}3d_{5/2}[4]3d_{3/2}$
$3d_{3/2}3d_{3/2}[2]3d_{5/2}$	$3p_{1/2}3p_{3/2}[2]3d_{5/2}$	$3d_{3/2}3d_{3/2}[2]3s_{1/2}$	
$3d_{5/2}3d_{5/2}[2]3d_{3/2}$	$3d_{3/2}3d_{3/2}[2]3s_{1/2}$	$3d_{5/2}3d_{5/2}[2]3s_{1/2}$	$3p_{3/2}3p_{3/2}[2]3d_{5/2}$
	$3d_{5/2}3d_{5/2}[2]3s_{1/2}$	$3d_{3/2}3d_{5/2}[2]3s_{1/2}$	$3p_{1/2}3p_{3/2}[2]3d_{5/2}$
	$3d_{3/2}3d_{5/2}[1]3s_{1/2}$	$3d_{3/2}3d_{5/2}[3]3s_{1/2}$	$3d_{5/2}3d_{5/2}[4]3s_{1/2}$
	$3d_{3/2}3d_{5/2}[2]3s_{1/2}$	$3d_{3/2}3d_{3/2}[0]3d_{5/2}$	$3d_{3/2}3d_{5/2}[4]3s_{1/2}$
	$3d_{3/2}3d_{3/2}[2]3d_{5/2}$	$3d_{3/2}3d_{3/2}[2]3d_{5/2}$	$3d_{3/2}3d_{3/2}[2]3d_{5/2}$
	$3d_{5/2}3d_{5/2}[0]3d_{3/2}$	$3d_{5/2}3d_{5/2}[2]3d_{3/2}$	$3d_{5/2}3d_{5/2}[4]3d_{3/2}$
	$3d_{5/2}3d_{5/2}[2]3d_{3/2}$	$3d_{5/2}3d_{5/2}[4]3d_{3/2}$	$3d_{5/2}3d_{5/2}[2]3d_{5/2}$
	$3d_{3/2}3d_{3/2}[0]3d_{3/2}$	$3d_{5/2}3d_{5/2}[0]3d_{5/2}$	
	$3d_{5/2}3d_{5/2}[2]3d_{5/2}$		$3d_{5/2}3d_{5/2}[4]3d_{3/2}$

and Al-like ions are due to the increased size of the model space ($3l3l'3l''$ instead of $2l2l'2l''$) and differences in the Dirac-Fock potential ($1s^22s^22p^6$ instead of $1s^2$). There are 148 states for Al-like ions compared with only 15 for B-like ions; consequently, the numerical calculations for aluminum-like ions are more laborious.

A. Model space

The model space for $n=3$ states of aluminumlike ions includes 75 odd-parity states consisting of 13 $J=1/2$ states, 22 $J=3/2$ states, 19 $J=5/2$ states, 13 $J=7/2$ states, six $J=9/2$ states, and two $J=11/2$ states. Additionally, there are

TABLE II. Contributions to energy matrices (a.u.) for odd-parity states with $J=1/2$ before diagonalization in the case of Al-like germanium, $Z=32$.

$3l_1j_13l_2j_2[J_{12}]3l_3j_3$	$3l_1j_13l_2j_2[J_{12}]3l_3j_3$	$E^{(0)}$	$E^{(1)}$	$B^{(1)}$	$E^{(2)}$
$3s_{1/2}3s_{1/2}[0]3p_{1/2}$	$3s_{1/2}3s_{1/2}[0]3p_{1/2}$	−95.286056	4.897918	0.043952	−0.167811
$3p_{3/2}3p_{3/2}[0]3p_{1/2}$	$3p_{3/2}3p_{3/2}[0]3p_{1/2}$	−91.239265	5.365837	0.046278	−0.225383
$3s_{1/2}3p_{1/2}[1]3d_{3/2}$	$3s_{1/2}3p_{1/2}[1]3d_{3/2}$	−90.910510	5.326804	0.041066	−0.233031
$3s_{1/2}3p_{3/2}[1]3d_{3/2}$	$3s_{1/2}3p_{3/2}[1]3d_{3/2}$	−90.636363	5.535290	0.034844	−0.252306
$3s_{1/2}3p_{3/2}[2]3d_{3/2}$	$3s_{1/2}3p_{3/2}[2]3d_{3/2}$	−90.636363	4.909723	0.035206	−0.188381
$3s_{1/2}3p_{3/2}[2]3d_{5/2}$	$3s_{1/2}3p_{3/2}[2]3d_{5/2}$	−90.586586	5.343152	0.031624	−0.229276
$3d_{3/2}3d_{3/2}[0]3p_{1/2}$	$3d_{3/2}3d_{3/2}[0]3p_{1/2}$	−86.534964	5.648678	0.039064	−0.272410
$3d_{3/2}3d_{3/2}[2]3p_{3/2}$	$3d_{3/2}3d_{3/2}[2]3p_{3/2}$	−86.260817	5.520663	0.031397	−0.265319
$3d_{5/2}3d_{5/2}[0]3p_{1/2}$	$3d_{5/2}3d_{5/2}[0]3p_{1/2}$	−86.435409	5.968196	0.032085	−0.317041
$3d_{5/2}3d_{5/2}[2]3p_{3/2}$	$3d_{5/2}3d_{5/2}[2]3p_{3/2}$	−86.161262	5.535474	0.024322	−0.257509
$3d_{3/2}3d_{5/2}[1]3p_{1/2}$	$3d_{3/2}3d_{5/2}[1]3p_{1/2}$	−86.485186	5.360735	0.035399	−0.240544
$3d_{3/2}3d_{5/2}[1]3p_{3/2}$	$3d_{3/2}3d_{5/2}[1]3p_{3/2}$	−86.211039	5.785456	0.029024	−0.295486
$3d_{3/2}3d_{5/2}[2]3p_{3/2}$	$3d_{3/2}3d_{5/2}[2]3p_{3/2}$	−86.211039	5.562748	0.027898	−0.272622
$3s_{1/2}3s_{1/2}[0]3p_{1/2}$	$3p_{3/2}3p_{3/2}[0]3p_{1/2}$	0.000000	−0.544408	−0.000662	0.040021
$3p_{3/2}3p_{3/2}[0]3p_{1/2}$	$3s_{1/2}3s_{1/2}[0]3p_{1/2}$	0.000000	−0.544408	−0.000662	0.037766
$3s_{1/2}3s_{1/2}[0]3p_{1/2}$	$3s_{1/2}3p_{1/2}[1]3d_{3/2}$	0.000000	0.400156	0.000212	−0.033861
$3s_{1/2}3p_{1/2}[1]3d_{3/2}$	$3s_{1/2}3s_{1/2}[0]3p_{1/2}$	0.000000	0.400156	0.000212	−0.030354
$3s_{1/2}3s_{1/2}[0]3p_{1/2}$	$3s_{1/2}3p_{3/2}[1]3d_{3/2}$	0.000000	−0.374459	−0.000294	0.030131
$3s_{1/2}3p_{3/2}[1]3d_{3/2}$	$3s_{1/2}3s_{1/2}[0]3p_{1/2}$	0.000000	−0.374459	−0.000294	0.027575
$3s_{1/2}3s_{1/2}[0]3p_{1/2}$	$3d_{3/2}3d_{3/2}[0]3p_{1/2}$	0.000000	0.209638	0.000372	−0.012544
$3d_{3/2}3d_{3/2}[0]3p_{1/2}$	$3s_{1/2}3s_{1/2}[0]3p_{1/2}$	0.000000	0.209638	0.000372	−0.007983
$3p_{3/2}3p_{3/2}[0]3p_{1/2}$	$3s_{1/2}3p_{3/2}[1]3d_{3/2}$	0.000000	0.300908	−0.000086	−0.027682
$3s_{1/2}3p_{3/2}[1]3d_{3/2}$	$3p_{3/2}3p_{3/2}[0]3p_{1/2}$	0.000000	0.300908	−0.000086	−0.027274
$3p_{3/2}3p_{3/2}[0]3p_{1/2}$	$3s_{1/2}3p_{3/2}[2]3d_{5/2}$	0.000000	0.376259	0.000134	−0.026256
$3s_{1/2}3p_{3/2}[2]3d_{5/2}$	$3p_{3/2}3p_{3/2}[0]3p_{1/2}$	0.000000	0.376259	0.000134	−0.025386
$3p_{3/2}3p_{3/2}[0]3p_{1/2}$	$3d_{3/2}3d_{3/2}[0]3p_{1/2}$	0.000000	−0.232469	−0.000433	0.020393
$3d_{3/2}3d_{3/2}[0]3p_{1/2}$	$3p_{3/2}3p_{3/2}[0]3p_{1/2}$	0.000000	−0.232469	−0.000433	0.017795
$3p_{3/2}3p_{3/2}[0]3p_{1/2}$	$3d_{5/2}3d_{5/2}[0]3p_{1/2}$	0.000000	−0.569116	−0.001312	0.043235
$3d_{5/2}3d_{5/2}[0]3p_{1/2}$	$3p_{3/2}3p_{5/2}[0]3p_{1/2}$	0.000000	−0.569116	−0.001312	0.039159

73 even-parity states consisting of 13 $J=1/2$ states, 21 $J=3/2$ states, 20 $J=5/2$ states, 11 $J=7/2$ states, 7 $J=9/2$ states, and one $J=11/2$ state. The distribution of the 148 states in the model space is given in Table I.

The evaluation of second-order energies for Al-like ions follows the pattern of the corresponding calculation for Mg-like ions given in Ref. [5]. In particular, we use second-order one- and two-particle matrix elements for Mg-like ions cal-

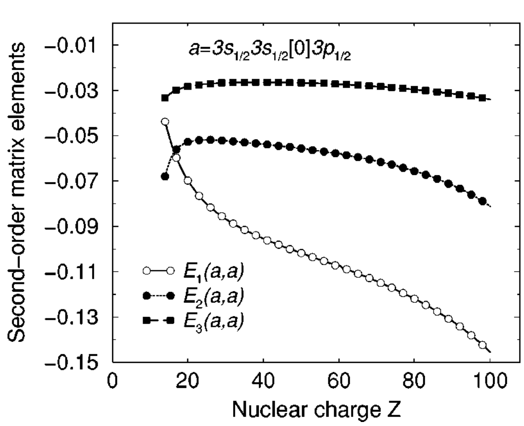

FIG. 1. One-, two-, and three-particle contributions E_1, E_2, and E_3 to the second-order diagonal energy matrix element for the $3s_{1/2}3s_{1/2}[0]3p_{1/2}$ state of Al-like ions given as functions of Z.

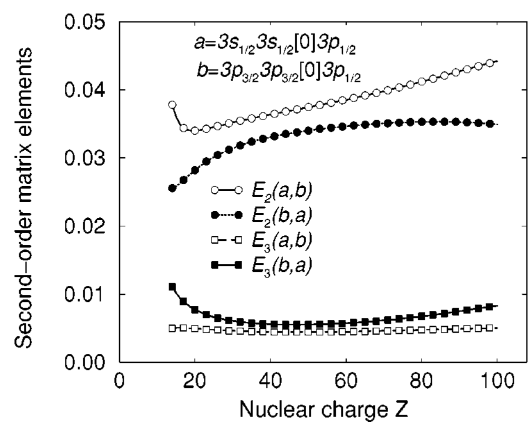

FIG. 2. Two- and three-particle contributions to nondiagonal second-order energy matrix for $3s_{1/2}3s_{1/2}[0]3p_{1/2}$ and $3p_{3/2}3p_{3/2}[0]3p_{1/2}$ states of Al-like ions given as functions of Z.

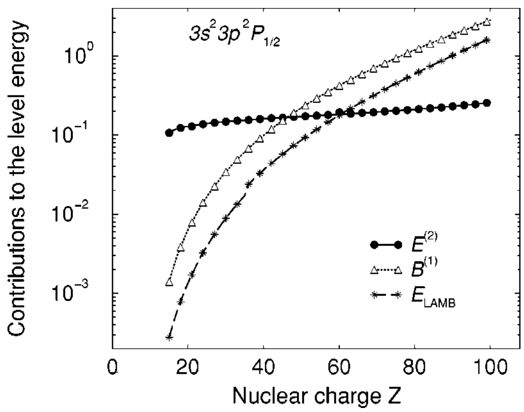

FIG. 3. Contributions to the energy of the $3s^2 3p\ ^2P_{1/2}$ ground state in Al-like ions from the second-order Coulomb energy $E^{(2)}$, the Breit interaction $B^{(1)}$, and the Lamb-shift $E_{\rm Lamb}$.

culated in [5], recoupled as described in [6], to obtain one- and two-particle contributions for Al-like ions. We refer the reader to Ref. [5] for a discussion of the how the basic one- and two-particle matrix elements are evaluated and to Ref. [6] for a discussion of how they are combined to obtain matrix elements for the three-particle system. A discussion of how intrinsic three-particle diagrams are evaluated and included is also given in [6]. The one-, two-, and three-particle matrix elements calculated here can be used later as input data for calculations of energies of four-valence-electron Si-like ions.

B. Energy-matrix elements

As a specific example of our calculations, we list the zeroth-, first-, and second-order Coulomb contributions $E^{(0)}$, $E^{(1)}$, and $E^{(2)}$, together with the first-order Breit contribution $B^{(1)}$, for the odd-parity $J=1/2$ states in aluminum-like germanium $Z=32$ in Table II. The zeroth-order Coulomb energy $E^{(0)}$, which is the sum of eigenvalues of the one-electron Dirac equation, dominates the energy matrix. The first-order Coulomb energy $E^{(1)}$ is the matrix element of the residual Coulomb interaction between the states listed in the first two columns. It is, as expected, the next most important contribution to the total energy. The second-order Coulomb energy $E^{(2)}$ is the sum of one-, two-, and three-particle contributions obtained using the standard rules of MBPT. The evaluation of $E^{(2)}$ is discussed in detail in Ref. [7] for the case of boronlike ions; the evaluation of $E^{(2)}$ for aluminumlike ions is similar. Finally, the first-order Breit energy $B^{(1)}$ is the matrix element of the retarded Breit interaction [24]

$$b_{12}=-\frac{1}{r_{12}}[\alpha_1\alpha_2\cos kr_{12}-(\alpha_1\nabla_1)(\alpha_2\nabla_2)\times(1-\cos kr_{12})/k^2]. \tag{2.1}$$

The quantity k in Eq. (2.1) is the wave vector of the virtual photon mediating the interaction; the choice of k for two-particle matrix elements is discussed in the Appendix of Ref. [25]. The first-order Breit corrections $B^{(1)}$ are smaller than the first- and second-order Coulomb corrections $E^{(1)}$ and $E^{(2)}$ for the example considered in Table II. Furthermore, the ratios of nondiagonal to diagonal matrix elements are smaller for first-order contributions than for second-order contributions. Another difference between first- and second-order contributions is symmetry: first-order nondiagonal matrix elements are symmetric whereas second-order nondiagonal matrix elements are unsymmetric; the matrix elements $E^{(2)}[v'w'[J'_{12}]u'(J),vw[J_{12}]u(J)]$ and $E^{(2)}[vw[J_{12}]u(J),v'w'[J'_{12}]u'(J)]$ in this example differ by 10–30 %.

The most difficult part of the calculation is the second-order Coulomb energy matrix which consists of three parts, associated with one-, two-, and three-particle operators. (Three-particle operators are, of course, absent for systems with one or two valence electrons.) In Fig. 1 we illustrate the Z dependence of the one-, two-, and three-particle second-order contributions E_1, E_2, and E_3 to the diagonal matrix element of the $3s_{1/2}3s_{1/2}[0]3p_{1/2}$ state. It can be seen from the figure that E_3 is almost constant for all Z. The two-

TABLE III. Energies of odd-parity $J=1/2$ states of Al-like germanium, $Z=32$, in a.u., $E^{(0+1)}\equiv E_0+E_1+B_1$. $E_{\rm rel}$ is the total theoretical energy relative to the ground state.

jj coupling	$E^{(0+1)}$	$E^{(2)}$	$E_{\rm Lamb}$	$E_{\rm tot}$	$E_{\rm rel}$
$3s_{1/2}3s_{1/2}[0]3p_{1/2}$	−90.482233	−0.150878	0.011710	−90.621401	0.000000
$3p_{3/2}3p_{3/2}[0]3p_{1/2}$	−86.079540	−0.200045	0.001639	−86.277946	4.343455
$3s_{1/2}3p_{1/2}[1]3d_{3/2}$	−85.870751	−0.189035	0.005944	−86.053842	4.567559
$3s_{1/2}3p_{3/2}[1]3d_{3/2}$	−85.723046	−0.184160	0.006253	−85.900953	4.720448
$3s_{1/2}3p_{3/2}[2]3d_{3/2}$	−84.978205	−0.253607	0.005793	−85.226019	5.395382
$3s_{1/2}3p_{3/2}[2]3d_{5/2}$	−84.832708	−0.275664	0.005708	−85.102665	5.518736
$3d_{3/2}3d_{3/2}[0]3p_{1/2}$	−81.101794	−0.240344	−0.000083	−81.342222	9.279179
$3d_{3/2}3d_{3/2}[2]3p_{3/2}$	−81.083557	−0.239941	−0.000082	−81.323580	9.297821
$3d_{5/2}3d_{5/2}[0]3p_{1/2}$	−80.843906	−0.239630	0.000343	−81.083194	9.538207
$3d_{5/2}3d_{5/2}[2]3p_{3/2}$	−80.734599	−0.260151	0.000179	−80.994571	9.626830
$3d_{3/2}3d_{5/2}[1]3p_{1/2}$	−80.583712	−0.272143	0.000327	−80.855528	9.765872
$3d_{3/2}3d_{5/2}[1]3p_{3/2}$	−80.330089	−0.313922	0.000183	−80.643828	9.977573
$3d_{3/2}3d_{5/2}[2]3p_{3/2}$	−79.738244	−0.397240	0.000320	−80.135164	10.486236

TABLE IV. Energies of Al-like ions relative to the ground state in cm^{-1} for ions with $Z=18$–36.

LS scheme	$Z=18$	$Z=20$	$Z=22$	$Z=24$	$Z=26$	$Z=28$	$Z=30$	$Z=36$	jj scheme
$3s^2[^1S]3p\ ^2P_{1/2}$	0	0	0	0	0	0	0	0	$3s_{1/2}3s_{1/2}[0]3p_{1/2}$
$3s^2[^1S]3p\ ^2P_{3/2}$	2209	4392	7534	12246	18831	27731	39441	97281	$3s_{1/2}3s_{1/2}[0]3p_{3/2}$
$3p^2[^3P]3s\ ^4P_{1/2}$	100321	135434	160310	192144	225187	259627	295565	411898	$3p_{1/2}3p_{1/2}[0]3s_{1/2}$
$3p^2[^3P]3s\ ^4P_{3/2}$	101119	137020	163161	196946	232889	271526	313401	464088	$3p_{1/2}3p_{3/2}[1]3s_{1/2}$
$3p^2[^3P]3s\ ^4P_{5/2}$	102350	139374	167202	203357	242451	285072	331743	500343	$3p_{1/2}3p_{3/2}[2]3s_{1/2}$
$3p^2[^1D]3s\ ^2D_{3/2}$	132057	176156	211458	253993	298903	346780	398202	579451	$3p_{1/2}3p_{3/2}[2]3s_{1/2}$
$3p^2[^1D]3s\ ^2D_{5/2}$	132160	176369	212003	255126	301126	350924	405567	611361	$3p_{3/2}3p_{3/2}[2]3s_{1/2}$
$3p^2[^1S]3s\ ^2S_{1/2}$	169813	220861	263850	313234	364267	417197	472400	657480	$3p_{1/2}3p_{3/2}[1]3s_{1/2}$
$3p^2[^3P]3s\ ^2P_{1/2}$	181937	236033	280335	332633	388057	447817	513114	754381	$3p_{3/2}3p_{3/2}[0]3s_{1/2}$
$3p^2[^3P]3s\ ^2P_{3/2}$	183325	238615	284491	338680	396052	457537	524114	764631	$3p_{3/2}3p_{3/2}[2]3s_{1/2}$
$3s^2[^1S]3d\ ^2D_{3/2}$	217980	283270	344199	407623	472279	538960	608425	842274	$3s_{1/2}3s_{1/2}[0]3d_{3/2}$
$3s^2[^1S]3d\ ^2D_{5/2}$	218030	283288	344726	408710	474242	542192	613395	855275	$3s_{1/2}3s_{1/2}[0]3d_{5/2}$
$3s3p[^3P]3d\ ^2D_{3/2}$	259555	340833	412733	492938	576065	662532	752665	1049206	$3s_{1/2}3p_{1/2}[0]3d_{3/2}$
$3s3p[^3P]3d\ ^2D_{5/2}$	259765	341308	413695	494898	579912	669745	765417	1097220	$3s_{1/2}3p_{1/2}[0]3d_{5/2}$
$3p^2[^3P]3p\ ^4S_{3/2}$	270375	351214	423261	504154	588844	678402	773983	1107265	$3p_{1/2}3p_{1/2}[0]3p_{3/2}$
$3s3p[^3P]3d\ ^4F_{3/2}$	290045	382170	463380	550911	641239	733529	828935	1141165	$3s_{1/2}3p_{1/2}[1]3d_{3/2}$
$3s3p[^3P]3d\ ^4F_{5/2}$	290489	383051	464938	554065	645313	739490	837352	1160608	$3s_{1/2}3p_{1/2}[1]3d_{3/2}$
$3s3p[^3P]3d\ ^4F_{7/2}$	291124	384321	467215	557844	651223	748302	849974	1190862	$3s_{1/2}3p_{1/2}[1]3d_{5/2}$
$3s3p[^3P]3d\ ^4F_{9/2}$	291968	386020	470300	563048	659539	761051	868882	1244203	$3s_{1/2}3p_{3/2}[2]3d_{5/2}$
$3p^2[^3P]3p\ ^2P_{1/2}$	293233	379299	461285	549476	641696	738981	842438	1201579	$3p_{3/2}3p_{3/2}[0]3p_{1/2}$
$3p^2[^3P]3p\ ^2P_{3/2}$	293209	379436	461846	551612	645244	745789	854345	1227316	$3p_{3/2}3p_{3/2}[2]3p_{1/2}$
$3s3p[^3P]3d\ ^4P_{1/2}$	316813	415750	503262	597441	693557	792568	895282	1232711	$3s_{1/2}3p_{1/2}[1]3d_{3/2}$
$3s3p[^3P]3d\ ^4P_{3/2}$	316328	414802	502037	596093	692051	790868	893409	1247406	$3s_{1/2}3p_{1/2}[1]3d_{5/2}$
$3s3p[^3P]3d\ ^4P_{5/2}$	315700	413738	500557	594205	689678	787889	889691	1225100	$3s_{1/2}3p_{1/2}[1]3d_{5/2}$
$3s3p[^3P]3d\ ^4D_{1/2}$	318711	417376	505957	602892	703197	808018	918540	1296841	$3s_{1/2}3p_{3/2}[1]3d_{3/2}$
$3s3p[^3P]3d\ ^4D_{3/2}$	318970	417939	506596	603407	703580	808276	918667	1296621	$3s_{1/2}3p_{3/2}[1]3d_{3/2}$
$3s3p[^3P]3d\ ^4D_{5/2}$	319206	418317	506976	603619	703500	807792	917656	1292121	$3s_{1/2}3p_{3/2}[1]3d_{3/2}$
$3s3p[^3P]3d\ ^4D_{7/2}$	319338	418427	506910	603232	702727	806675	916341	1293028	$3s_{1/2}3p_{3/2}[1]3d_{5/2}$
$3p^2[^3P]3p\ ^2D_{3/2}$	328864	428446	518071	615700	716538	821780	932599	1309701	$3p_{3/2}3p_{3/2}[0]3p_{3/2}$
$3p^2[^3P]3p\ ^2D_{5/2}$	328820	428429	518144	615972	717163	822910	934224	1303206	$3p_{3/2}3p_{3/2}[2]3p_{1/2}$
$3s3p[^3P]3d\ ^2F_{5/2}$	343349	448090	541512	641668	743733	848841	958273	1335418	$3s_{1/2}3p_{3/2}[1]3d_{5/2}$
$3s3p[^3P]3d\ ^2F_{7/2}$	345106	451501	547483	651360	758566	870461	988375	1392067	$3s_{1/2}3p_{3/2}[2]3d_{3/2}$
$3s3p[^3P]3d\ ^2P_{1/2}$	376441	489957	591712	701320	814018	931184	1054121	1470443	$3s_{1/2}3p_{3/2}[2]3d_{3/2}$
$3s3p[^3P]3d\ ^2P_{3/2}$	375966	488541	589105	696596	806112	918700	1035340	1420903	$3s_{1/2}3p_{3/2}[1]3d_{5/2}$
$3s3p[^1P]3d\ ^2F_{5/2}$	375645	490767	594392	705300	818947	936625	1059562	1472503	$3s_{1/2}3p_{3/2}[2]3d_{3/2}$
$3s3p[^1P]3d\ ^2F_{7/2}$	375157	489885	592959	703154	815939	932647	1054581	1465653	$3s_{1/2}3p_{3/2}[2]3d_{5/2}$
$3s3p[^1P]3d\ ^2P_{1/2}$	390186	505823	610461	722770	837739	956613	1080651	1497768	$3s_{1/2}3p_{3/2}[2]3d_{5/2}$
$3s3p[^1P]3d\ ^2P_{3/2}$	390093	505935	610978	723763	839172	958617	1083786	1509620	$3s_{1/2}3p_{3/2}[2]3d_{3/2}$
$3s3p[^1P]3d\ ^2D_{3/2}$	395132	510442	614764	726764	842226	962572	1088959	1518779	$3s_{1/2}3p_{3/2}[2]3d_{5/2}$
$3s3p[^1P]3d\ ^2D_{5/2}$	395438	511035	615681	727926	843273	963132	1088896	1516157	$3s_{1/2}3p_{3/2}[2]3d_{5/2}$

particle contribution is largest for low-Z ions; however, with increasing Z, the one-particle contribution becomes more important. As a result, the ratio of the three-particle energy E_3 to the total second-order energy $E^{(2)}$ decreases slowly with increasing Z.

In Fig. 2, we give two- and three-particle contributions to the nondiagonal elements $E_i(a,b)$ and $E_i(b,a)$, $i=2,3$, where $a=3s_{1/2}3s_{1/2}[0]3p_{1/2}(1/2)$ and $b=3p_{3/2}3p_{3/2}[0]3p_{1/2}(1/2)$, as an example. The origin of the asymmetry of the nondiagonal second-order matrix elements in MBPT calculations was discussed previously in Ref. [26].

C. Eigenvalues and eigenvectors for Al-like ions

After evaluating the energy matrices, we calculate eigenvalues and eigenvectors for states with given values of J and parity. There are two possible methods to carry out the diagonalization: (a) diagonalize the sum of zeroth- and first-order matrices, then calculate the second-order contributions using the resulting eigenvectors; or (b) diagonalize the sum of the zeroth-, first-, and second-order matrices together. Following Ref. [6], we choose the second method here. We find that the energies are smooth, slowly varying functions of Z for the 148 levels of Al-like ions. It is simple to identify the

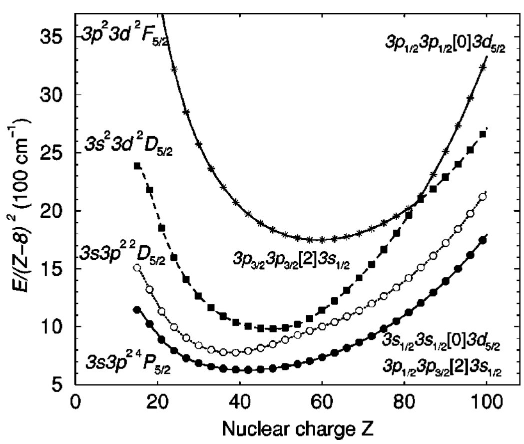

FIG. 4. Energies $[E/(Z-8)^2$ in 100 cm$^{-1}]$ of odd-parity states with $J=5/2$ as functions of Z.

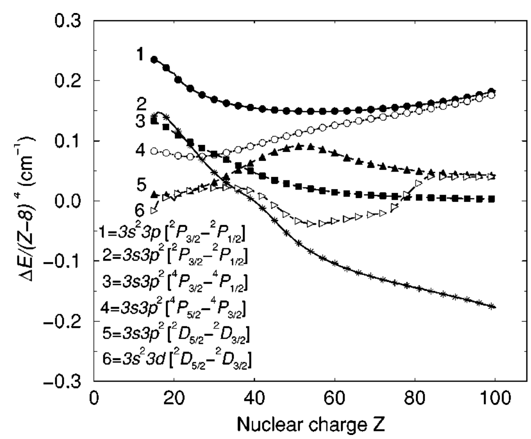

FIG. 5. Multiplet splitting energies $[\Delta E/(Z-8)^4$ in cm$^{-1}]$ as functions of Z.

doublet $3s^2 3p\ ^2P$ and quartet $3s3p^2\ ^4P$ states for low-Z ions. We find that the splitting of the doublet and quartet states is comparable to the difference between LS terms for high-Z ions; consequently, it is not possible to use the LS designation for high-Z ions. In fact, we obtain almost pure jj coupling for the highest values of Z.

The relative importance of second-order contributions to energies is illustrated in Fig. 3, where the variation with Z of the second-order energy $E^{(2)}$, the first-order Breit energy $B^{(1)}$, and the QED contribution $E_{\rm Lamb}$ are shown for the $3s^2 3p\ ^2P_{1/2}$ ground state. As shown in Fig. 3, $E^{(2)}$ is the dominant correction for $Z<46$. The QED correction $E_{\rm Lamb}$ is smaller than $B^{(1)}$ by a factor of 2–5 for all Z but is larger than $E^{(2)}$ for $Z\geqslant 60$.

In Table III, we give the following contributions to the energies of 13 excited odd-parity $J=1/2$ states in Ge^{19+}: $E^{(0+1)}=E^{(0)}+E^{(1)}+B^{(1)}$, the second-order Coulomb energy $E^{(2)}$, the QED correction $E_{\rm Lamb}$, and the total theoretical energy $E_{\rm tot}$. The QED correction is the sum of the one-particle self-energy and the first-order vacuum-polarization energy. Screened self-energy and vacuum-polarization data given by Blundell [4] are used here to determine the QED correction $E_{\rm Lamb}$. The table clearly shows the importance of including second-order contributions.

We also present the theoretical excitation energy $E_{\rm rel}$ relative to the $3s^2 3p\ ^2P_{1/2}$ ground state in Table III. As can be seen, the excitation energy increases with increasing number of one-particle $3d$ states in the dominant configuration. Indeed, the odd-parity $J=1/2$ levels in this table can be divided into two groups according to the number of $3d$ states: those with energies less than 5.7 a.u. have zero or one $3d$ state and those with energies larger than 9 a.u. have two $3d$ states. Even-parity $J=1/2$ levels also fall into two groups: those with zero or one $3d$ electron have energies less than 3.2 a.u and those with two or three $3d$ electrons have energies greater than 6 a.u. Levels with values of $J>1/2$ fall into the same two distinct groups as those with $J=1/2$: low-excitation-energy states with zero or one $3d$ electron and high-excitation-energy states with two or three $3d$ electrons. The first group includes the 40 levels $3s_{1/2}3s_{1/2}[0]3p_j(J)$, $3s_{1/2}3p_j[J_{12}]3d_{j'}(J)$, $3s_{1/2}3s_{1/2}[0]3d_j(J)$, and $3s_{1/2}3p_j[J_{12}]3p_{j'}(J)$ levels, and the second group includes the remaining 108 levels $3d_j3d_{j'}[J_{12}]3p_{j''}(J)$, $3p_j3p_{j'}[J_{12}]3d_{j''}(J)$, and $3d_j3d_{j'}[J_{12}]3d_{j''}(J)$. The first group of levels has been studied experimentally, whereas there are no experimental data for the second group. Below, we discuss the first group of levels only. For these 40 levels, we use both jj designations and LS designations. When starting calculations from relativistic Dirac-Fock wave functions, it is natural to use jj designations for uncoupled energy matrix elements; however, neither jj nor LS coupling describes *physical* states properly, except for the single-configuration state $3d_{5/2}3d_{5/2}(4)3d_{3/2}\equiv 3d^3\ ^3G_{11/2}$. Both designations are given in Table IV where we summarize our energy calculations for the 40 low-lying levels.

Strong mixing between states inside the even-parity complex with $J=3/2$ and 5/2 was discussed by Ekberg *et al.* in Ref. [8] and by Jupén and Curtis in Ref. [9]. Additionally, we found strong mixing inside the odd-parity complex with $J=1/2$–5/2 and the even-parity complex with $J=1/2$. In particular, strong mixing is found in the even-parity complex with $J=5/2$ between $3p_{1/2}3p_{3/2}[2]3s_{1/2}$ and $3p_{3/2}3p_{3/2}[2]3s_{1/2}$ states for $Z=27$–28, between $3p_{3/2}3p_{3/2}[2]3s_{1/2}$ and $3s_{1/2}3s_{1/2}[0]3d_{3/2}$ states for $Z=53$–54, and between $3p_{3/2}3p_{3/2}[2]3s_{1/2}$ and $3p_{1/2}3p_{1/2}[0]3d_{3/2}$ states for $Z=83$–84. It can be seen from Table I that the even-parity complex with $J=5/2$ includes two $3p_j3p_{j'}[2]3s_{1/2}$ states, one $3s_{1/2}3s_{1/2}[0]3d_{5/2}$ state, eight $3p_j3p_{j'}[J_{12}]3d_{j''}$ states, four $3d_j3d_{j'}[J_{12}]3s_{1/2}$ states, and five $3d_j3d_{j'}[J_{12}]3d_{j''}$ states. The resulting 20 eigenvalues can be simply enumerated or labeled using LS or jj schemes. We label the first four levels as $3s3p^2\ ^4P_{5/2}$, $3s3p^2\ ^2D_{5/2}$, $3s^2 3d\ ^2D_{5/2}$, and $3p^2 3d\ ^2F_{5/2}$, respectively. Only three mixing coefficients suffice to describe the $3s3p^2\ ^2D_{5/2}$ level. To describe the next level $3s^2 3d\ ^2D_{5/2}$, one additional mixing coefficient is needed. It is much more complicated to describe the fourth level $3p^2 3d\ ^2F_{5/2}$, since nine mixing coefficients have values greater than 0.1 for low-Z ions. It should be noted that the energy of the $3s^2 3d\ ^2D_{5/2}$ level is almost equal to the energy of the $3p^2 3d\ ^2F_{5/2}$ level for $Z=83$. The energies of the

TABLE V. Fine-structure splitting (in cm^{-1}) of the $3s^2 3p\ ^2P$ and $3s3p^2\ ^4P$ terms in Al-like ions with $Z=15$–42. Comparison of the MBPT and predicted data.

Z	$3s^23p[^2P_{3/2}$-$^2P_{1/2}]$ MBPT	NIST	$3s3p^2\ [^4P_{3/2}$-$^4P_{1/2}]$ MBPT	NIST	Fit [a]	$3s3p^2\ [^4P_{5/2}$-$^4P_{3/2}]$ MBPT	NIST	Fit [a]	$3s3p^2\ [^4P_{5/2}$-$^4P_{1/2}]$ MBPT	Fit [a]
15	564	559 [c]	198	204 [c]	204	320	328 [c]	328	518	532
16	950	951 [d]	331	331 [d]	343	526	520 [d]	548	857	891
17	1493		536		537	840		845	1376	1382
18	2209		798		802	1231		1235	2029	2037
19	3134	3134 [e]	1141	1136 [e]	1053	1730	1737 [e]	1829	2871	2882
20	4392	4309 [e]	1586	1578 [e]	1428	2354	2364 [e]	2524	3940	3952
21	5755	5761 [e]	2146	2122 [e]	1919	3120	3157 [e]	3364	5266	5283
22	7534	7543 [e]	2852	2805 [e]	2562	4041	4109 [e]	4349	6893	6911
23	9682	9696 [f]	3727	3711 [f]	3392	5134	5151 [f]	5485	8861	8877
24	12246	12261 [g]	4802	4789 [g]	4442	6411	6434 [g]	6783	11213	11225
25	15278	15295 [h]	6114	6107 [h]	5758	7884	7913 [h]	8241	13998	13999
26	18831	18852 [i]	7702	7710 [i]	7387	9562	9596 [i]	9862	17264	17249
27	22962	22979 [j]	9613	9571 [j]	9373	11449	11471 [j]	11654	21062	21027
28	27731	27770 [e]	11899		11775	13545		13611	25444	25386
29	33201	33239 [k]	14618	14579 [k]	14645	15846	15898 [k]	15738	30464	30383
30	39441	39483 [l]	17835	17793 [l]	18044	18342	18366 [l]	18035	36177	36079
31	46520		21624		22035	21017		20502	42641	42537
32	54512	54567 [b]	26062	26027 [b]	26697	23851	23975 [b]	23127	49913	49824
33	63497		31237		32073	26818		25935	58055	58008
34	73555	73626 [b]	37244	37243 [b]	38276	29891	30056 [b]	28887	67135	67163
35	84772		44181		45348	33042		32016	77223	77364
36	97281	97312 [m]	52190	51960 [m]	53397	36255	36190 [m]	35293	88445	88690
37	111095		61323		62511	39480		38714	100803	101225
38	126350	126414 [b]	71728	71909 [b]	72773	42706	42981 [b]	42282	114434	115055
39	143149	143211 [b]	83530	83809 [b]	84279	45917	46236 [b]	45990	129447	130269
40	161599	161680 [b]	96858	97257 [b]	97134	49098	49462 [b]	49827	145956	146961
41	181813		111845		111471	52241		53757	164086	165228
42	203906	204020 [n]	128628		127363	55340		57808	183968	185171

[a] Jupén and Curtis [9].
[b] Ekberg *et al.* [8].
[c] Martin *et al.* [11].
[d] Martin *et al.* [12].
[e] Sugar and Corliss [13].
[f] Shirai *et al.* [14].
[g] Shirai *et al.* [15].
[h] Shirai *et al.* [16].
[i] Shirai *et al.* [17].
[j] Shirai *et al.* [18].
[k] Sugar and Mosgrove [19].
[l] Sugar and Musgrove [20].
[m] Shirai *et al.* [22].
[n] Sugar and Musgrove [23].

$3s^23d\ ^2D_{5/2}$ and $3p^23d\ ^2F_{5/2}$ levels are 11 658 385 cm^{-1} and 11 645 413 cm^{-1}, respectively, with a difference of 12 972 cm^{-1}, which is about 0.1% of the level energies. A corresponding sharp change in the mixing coefficient $C(3p_{3/2}3p_{3/2}[2]3s_{1/2})$ at $Z=83$ is found.

Energies of even-parity states with $J=5/2$ relative to the ground state, divided by $(Z-8)^2$, are shown in Fig. 4. We already mentioned that the even-parity complex with $J=5/2$ includes 20 $3l3l'[J_{12}]3l''$ states. Energies of the four lowest levels are shown in Fig. 4, where we use LS designations for small Z and jj for large Z.

III. COMPARISON OF RESULTS WITH OTHER THEORY AND EXPERIMENT

We calculated energies of the 75 odd-parity states and the 73 even-parity excited states for Al-like ions with nuclear charges ranging from $Z=14$ to 100. In Table IV, we illustrate our theoretical results for the energies of the 30 low-lying odd-parity states. These states are $3s_{1/2}3s_{1/2}[0]3p_j(J)$, $3s_{1/2}3p_j[J_{12}]3d_{j'}(J)$, and $3p_j3p_{j'}[J_{12}]3p_{j''}(J)$ in jj coupling or $3s^23p\ ^2P_J$, $3s3p3d\ ^{2S+1}L_J$, and $3p^3\ ^{2S+1}L_J$ in LS coupling. We also give the energies of the ten low-lying even-parity states. These states are $3p_j3p_{j'}[J_{12}]3s_{1/2}(J)$ and

$3s_{1/2}3s_{1/2}[0]3d_j(J)$ in jj coupling or $3s3p^2\ ^{2S+1}L_J$ and $3s^23d\ ^2D_J$ in LS coupling. Calculations are presented for Al-like ions with nuclear charges ranging from $Z=18$ to 36. We limited the number of states and ions to compare with other results and experimental data. Our comparison is presented in two parts: transition energies and fine-structure energy differences.

A. Transition energies

Comparisons of our MBPT energies with other theoretical and experimental data are too voluminous to include here but are available as supplementary data in Ref. [27]. Predicted data based on measurements has been given by Martin *et al.* in Ref. [11] for P^{2+} and in Ref. [12] for S^{3+}. Similar data for Fe^{13+} were given by Shirai *et al.* in Ref. [17]. Our results are in good agreement with the predicted data, the difference being 0.3–0.5 % for most cases. It should be noted that relativistic MBPT calculations are more accurate for high-Z ions. Good agreement with experimental data obtained for low-Z ions leads us to conclude that the MBPT method can provide accurate energies for all values of Z. Ekberg *et al.* gave energies of $3s^23p\ ^2P_J$, $3s3p3d\ ^{2S+1}L_J$, $3s3p^2\ ^{2S+1}L_J$, and $3s^23d\ ^2D_J$ states of Al-like ions with nuclear charges ranging from $Z=32$ to 40 in Ref. [8]. The values in [8] were determined from the observed transitions in a stepwise fitting procedure. The differences between the observed energies and the theoretically calculated values using the Grant codes were fitted using a polynomial representation to obtain smoothed energies. Our MBPT results are in excellent agreement with adopted data from [8], the difference being about 0.01–0.1 % for most cases. The $3s^23p\ ^2P$–$3s3p^2\ ^4P$ transitions in Al-like ions P^{2+}–Mo^{29+} were investigated in a recently published paper by Jupén and Curtis [9]. We find some differences with that work as discussed in the following subsection.

B. Fine structure of the ^2L and ^4L terms

In Fig. 5, we present the fine-structure splitting scaled as $(Z-8)^4$ for the four doublet terms ($3s^23p\ ^2P$, $3s3p^2\ ^2P$, $3s3p^2\ ^2D$, $3s^23d\ ^2D$) and one quartet term ($3s3p^2\ ^4P$). The fine structure of the $3s3p^2\ ^4P$ term follows the Landé interval rules for low-Z ions; however, for high-Z ions ($Z>30$) the value of the $3s3p^2\ [^4P_{5/2}$-$^4P_{3/2}]$ splitting is smaller than the value of the $3s3p^2\ [^4P_{3/2}$-$^4P_{1/2}]$ splitting. As can be seen from Fig. 5, the $3s3p^2\ ^2P$ splitting is inverted for high-Z ions ($Z>38$); the $3s^23d\ ^2D$ splitting is inverted twice, at $Z=44$ and $Z=76$. The unusual splittings are due principally to changes from LS to jj coupling, with mixing from other doublet and quartet states. Further experimental confirmation would be very helpful in verifying the correctness of these occasionally sensitive mixing parameters.

In Table V, we compare results for the three fine-structure intervals $3s^23p[^2P_{3/2}$-$^2P_{1/2}]$, $3s3p^2\ [^4P_{3/2}$-$^4P_{1/2}]$, and $3s3p^2\ [^4P_{5/2}$-$^4P_{3/2}]$ in Al-like ions with $Z=15$–42. Our MBPT values are compared with predicted data given by Jupén and Curtis in Ref. [9], by Ekberg *et al.* in Ref. [8], and by researchers at the National Institute of Standards and Technology (NIST) in Refs. [11–23]. As can be seen from Table V, there is disagreement between the MBPT and values predicted by Jupén and Curtis in Ref. [9] for the $3s3p^2\ [^4P_{3/2}$-$^4P_{1/2}]$ and $3s3p^2\ [^4P_{5/2}$-$^4P_{3/2}]$ intervals. On the other hand, the MBPT energies agree very well with those from the tabulations of [11–23] for the above mentioned intervals and for the $3s^23p[^2P_{3/2}$-$^2P_{1/2}]$ interval. In the two last columns of Table V, we compare the MBPT energies with results from Ref. [9] for the $3s3p^2\ [^4P_{5/2}$-$^4P_{1/2}]$ interval. We see from this table that the comparison for the $3s3p^2\ [^4P_{5/2}$-$^4P_{1/2}]$ interval is much better than those for the $3s3p^2\ [^4P_{3/2}$-$^4P_{1/2}]$ and $3s3p^2\ [^4P_{5/2}$-$^4P_{3/2}]$ intervals. We conclude that the $3s3p^2\ ^4P_{3/2}$ level should be shifted in Ref. [9], to obtain reasonable agreement with the present theoretical results and the NIST data in [13–22].

IV. CONCLUSION

In summary, a systematic second-order MBPT study of the energies of the $n=3$ states of Al-like ions has been presented. The MBPT gives excellent agreement with experimental data and adopted results. It would be beneficial if experimental data for other highly charged Al-like ions were available. At the present time, there are no experimental data between $Z=43$ and $Z=100$ for the aluminum isoelectronic sequence. Availability of such data would lead to an improved understanding of the relative importance of different contributions to the energies of highly charged ions. These calculations provide a theoretical benchmark for comparison with experiment and theory. The results could be further improved by including third-order correlation corrections.

ACKNOWLEDGMENTS

The work of W.R.J. and M.S.S. was supported in part by National Science Foundation Grant No. PHY-99-70666. U.I.S. acknowledges partial support by Grant No. B503968 from Lawrence Livermore National Laboratory. The work of J.R.A. was performed under the auspices of the U.S. Department of Energy at the University of California, Lawrence Livermore National Laboratory under Contract No. W-7405-Eng-48. U.I.S. would also like to thank the members of the Data and Planning Center, the National Institute for Fusion Science, for their hospitality, friendly support, and many interesting discussions.

[1] K.-N. Huang, At. Data Nucl. Data Tables **34**, 1 (1986).
[2] B. C. Fawcett, At. Data Nucl. Data Tables **28**, 557 (1983).
[3] A. Farrag, E. Luc-Koenig, and J. Sinzelle, At. Data Nucl. Data Tables **27**, 539 (1982).
[4] S. A. Blundell, Phys. Rev. A **47**, 1790 (1993).
[5] U. I. Safronova, W. R. Johnson, and H. G. Berry, Phys. Rev. A **61**, 052503 (2000).
[6] M. S. Safronova, W. R. Johnson, and U. I. Safronova, Phys. Rev. A **54**, 2850 (1996).
[7] U. I. Safronova, W. R. Johnson, and M. S. Safronova, At. Data Nucl. Data Tables **69**, 183 (1998).
[8] J. O. Ekberg, A. Redfors, M. Brown, U. Feldman, and J. F. Seely, Phys. Scr. **44**, 539 (1991).
[9] C. Jupén and J. Curtis, Phys. Scr. **53**, 312 (1996).
[10] W. C. Martin and R. Zalubas, J. Phys. Chem. Ref. Data **12**, 323 (1983).
[11] W. C. Martin, R. Zalubas, and A. Musgrove, J. Phys. Chem. Ref. Data **14**, 751 (1985).
[12] W. C. Martin, R. Zalubas, and A. Musgrove, J. Phys. Chem. Ref. Data **19**, 821 (1990).
[13] J. Sugar and Ch. Corliss, J. Phys. Chem. Ref. Data **14**, Suppl. 2 (1985).
[14] T. Shirai, T. Nakagaki, J. Sugar, and W. L. Wiese, J. Phys. Chem. Ref. Data **21**, 273 (1992).
[15] T. Shirai, Y. Nakai, T. Nakagaki, J. Sugar, and W. L. Wiese, J. Phys. Chem. Ref. Data **22**, 1279 (1993).
[16] T. Shirai, T. Nakagaki, K. Okazaki, J. Sugar, and W. L. Wiese, J. Phys. Chem. Ref. Data **23**, 179 (1994).
[17] T. Shirai, Y. Funatake, K. Mori, J. Sugar, W. L. Wiese, and Y. Nakai, J. Phys. Chem. Ref. Data **19**, 127 (1990).
[18] T. Shirai, A. Mengoni, Y. Nakai, K. Mori, J. Sugar, W. L. Wiese, K. Mori, and N. Sakai, J. Phys. Chem. Ref. Data **21**, 23 (1992).
[19] J. Sugar and A. Musgrove, J. Phys. Chem. Ref. Data **19**, 527 (1990).
[20] J. Sugar and A. Musgrove, J. Phys. Chem. Ref. Data **24**, 1803 (1995).
[21] J. Sugar and A. Musgrove, J. Phys. Chem. Ref. Data **22**, 1213 (1993).
[22] T. Shirai, K. Okazaki, and J. Sugar, J. Phys. Chem. Ref. Data **24**, 1577 (1995).
[23] J. Sugar and A. Musgrove, J. Phys. Chem. Ref. Data **17**, 155 (1988).
[24] J. B. Mann and W. R. Johnson, Phys. Rev. A **4**, 44 (1971).
[25] M. H. Chen, K. T. Cheng, and W. R. Johnson, Phys. Rev. A **47**, 3692 (1993).
[26] M. S. Safronova, W. R. Johnson, and U. I. Safronova, J. Phys. B **30**, 2375 (1997).
[27] See EPAPS Document No. E-PLRAAN-65-002202 including the following five tables. Energies of Al-like ions relative to the ground state for ions with $Z=15$, 16, and 26. Energies of Al-like ions relative to the ground state in cm^{-1} for ions with $Z=32$, 34, 38–40. Energies of Al-like ions relative to the ground state in cm^{-1} for ions with $Z=17$–25, 27–31, 33, 35–37. Energies of the $3s^23p\ {}^2P_J$–$3s3p^2\ {}^4P_{J'}$ transitions as functions of Z. This document may be retrieved via the EPAPS homepage (http://www.aip.org/pubservs/epaps.html) or from ftp.aip.org in the directory /epaps/. See the EPAPS homepage for more information.